DOI: 10.1002/adsc.200700374

Development of a Q2MM Force Field for the Silver(I)-Catalyzed Hydroamination of Alkynes

Patrick J. Donoghue,[a] Elsa Kieken,[a] Paul Helquist,[a] and Olaf Wiest[a,*]

[a] Department of Chemistry and Biochemistry, University of Notre Dame, Notre Dame, Indiana 46556-5670, USA
Fax: (+1)-574-631-6652; e-mail: owiest@nd.edu

Received: July 27, 2007; Published online: November 21, 2007

Dedicated to our very good friend Jan-Erling Bäckvall on the occasion of his 60th birthday.
Grattis på födelsedagen!

Supporting information for this article is available on the WWW under http://asc.wiley-vch.de/home/.

Abstract: The intramolecular hydroamination of carbon-carbon π-bonds is an effective method for the rapid construction of nitrogen heterocycles. The rapid evaluation of suitable ligands using virtual screening will aid in the development of a stereoselective analogue of the reaction by predicting effective substrate/ligand combinations. Electronic structure calculations of the relevant transition structures for different nucleophiles and alkynes at the B3LYP/LACVP* level of theory are presented. They provide the basis for the development of a transition state force field by the Q2MM method, which is discussed in detail. The parameter development and performance for the transition state force field is presented.

Keywords: addition to alkynes; amines; hydroamination; molecular mechanics; silver

Introduction

The correct choice of a chiral ligand to achieve high enantioselectivity remains a key challenge in transition metal-catalyzed chemistry that has implications in many areas including the synthesis of pharmaceutically active compounds. The problem of optimizing catalyst selectivity shares many characteristics with the problems of drug design, where ligand binding to a target is optimized in the presence of other boundary conditions. Computational methods such as virtual screening have become indispensable tools of modern medicinal chemistry that complement the more traditional experimental approaches.[1,2] In principle, the methods developed in medicinal chemistry could be valuable tools in exploiting mechanistic information for the design and selection of chiral ligands for transition metal-catalyzed stereoselective synthesis.

The difficulty in applying the method of virtual screening to catalyst design is that the selectivity determining species is typically a transition state involving bond breaking and making, which normally requires treatment by quantum mechanical methods that are impractical for conformational sampling or the screening of even a small library of catalyst candidates. On the other hand, only the relative energies of the diastereomeric transition states are needed. This realization led to the development of much faster, reaction specific force fields for the calculation of stereoselecting transition states based on the reparameterization of force fields based on quantum mechanical results.[3] Such a development of reaction specific transition state force fields generally requires considerable effort by expert users, but the prospect of fast and reliable prediction of the enantioselectivity of reactions is sufficiently attractive to induce considerable effort in this area.[4]

New approaches suggest that the parameterization process could be automated by the Q2MM method developed by Norrby.[5,6] The unknown parameters of a force field are fitted to reproduce a set of reference data, for example, from *ab initio* calculations or X-ray structures. These reference data can include atomic charges, geometries, relative energies, and Hessian matrix values for parent and substituted cases. The very large number of reference data points ensures that even for large numbers of parameters to be fitted, the over-fitting criticized in the early days of reaction-specific force field fitting[7] will not be a problem. The quality of the fit is evaluated by a merit function, X^2, calculated from the squares of all devia-

tions of calculated values y_j from the reference values y_0 [Eq. (1)]. The deviations, multiplied by a weighting

$$x^2 = \sum_j w_i^2 (y_j - y_0)^2 \quad (1)$$

factor w_j that is based on the contribution of a parameter type to the total energy, are then minimized. A combination of modified Simplex and Newton–Raphson optimization procedures was shown to be the most successful in a series of test cases.[3c] We have optimized and parallelized the code for the fitting procedure to the point that it is fairly robust and allows the generation of a reaction specific force field within a few days. Transition state force fields derived by the Q2MM method have been successful in rationalizing and predicting the experimentally observed stereoselectivities for a number of reactions.[8]

Many biologically important compounds contain nitrogen heterocycles.[9] The synthesis of these heterocycles is therefore of particular interest. A promising strategy towards such heterocycles is the intramolecular hydroamination of alkenes and alkynes by an amine or amine derivative. Many different metal catalysts have been investigated for hydroamination of alkenes and alkynes, including lanthanides,[10] transition metals,[11] and some alkali earth metals.[12] Recently, we demonstrated the efficient catalysis of intramolecular hydroaminations of alkynes by silver 1,10-phenanthroline complexes.[13,14] Previous studies showed that phenanthroline can be a useful scaffold for chiral substituted derivatives that can easily be synthesized through the SmI_2-promoted coupling of phenanthroline with chiral ketones, aldehydes and epoxides.[15] Given the generality of the reaction, the question arises which of the chiral moieties chosen from any number of commercially available ketones, aldehydes or epoxides would give the most suitable ligand for enantioselective hydroamination. A library of these ligands could be prepared, but the task would be expensive both in cost of chiral materials and in the time needed to synthesize, purify, characterize, and screen all possible ligands. Clearly, a pre-selection of promising ligands would be desirable.

In this paper, we describe the development of a Q2MM force field for the transition structures of the silver-catalyzed hydroamination of alkynes that will be amenable to rapid prediction of the enantioselectivity for a given ligand/substrate combination. We will start our discussion by briefly describing the mechanism of the silver-catalyzed hydroamination and the results from the electronic structure calculations of the relevant transition structures. We will then outline the procedure used for the fitting of the transition state force field and discuss its performance by comparison with the reference data

Results and Discussion

The kinetics of the silver-catalyzed addition of amines to π-bonds has been studied in detail by Müller and co-workers.[16] In short, two competing sites are available for binding of the catalyst: σ-type binding to the amine represents the resting state, while the π-complex represents the catalytically active form. In the π-complex of alkyne substrates, the silver complexation activates the triple bond towards nucleophilic attack by an amine, emphasizing the increased reactivity of alkynes over alkenes, which are much less reactive due to the backbonding of the occupied orbitals on silver into the π* orbital of the olefin. After formation of the carbon-nitrogen bond, proton transfer to the α-carbon completes the hydroamination reaction and can potentially be mediated by the counterion of the silver.[17]

In order to develop the necessary MM parameters, several structures were calculated using QM methods at the B3LYP level. All of these structures are transition states for the addition of the amine to the silver-alkyne complex with a phenanthroline ligand. Nine such complexes were calculated, with various substituents on the amine, alkyne and phenanthroline. These complexes, numbered **1**–**9**, are schematically shown in Figure 1 and are combinations of ammonia, methylamine or ethylamine for the amine group, acetylene or propyne as the alkyne, and phenanthroline or 2-methylphenanthroline for the ligand. These model systems were selected to investigate different possibilities of regioselectivities and to investigate the steric factors governing them. The substructure for which the transition state force field parameters will be developed and its atom labels are shown in Figure 2.

For comparison, a ground state silver alkyne complex, **10**, was also calculated. The calculated structure of **1** is shown alongside the calculated structure of **10** in Figure 3, selected bond lengths are described in Table 1, and selected angles and dihedrals are described in Table 2. The ground state complex is highly symmetrical. In **10**, the Ag–N bonds are 2.32 Å, and the Ag–C bonds are 2.35 Å. Due to the silver binding, the acetylene is no longer linear, but the C–C–H bonds now have an angle of 170°. The C≡C bond is 1.22 Å, which suggests a π-bound alkyne and not a metallocyclopropene ring. The complex is also planar, with the alkyne parallel to the phenanthroline ligand.

Attack of the nitrogen nucleophile breaks the symmetry. As can be seen from the transition structure geometry in Figure 3, the free electron pair of the nitrogen donates into the antibonding orbital of the carbon-silver bond. As a result, the Ag–C distances

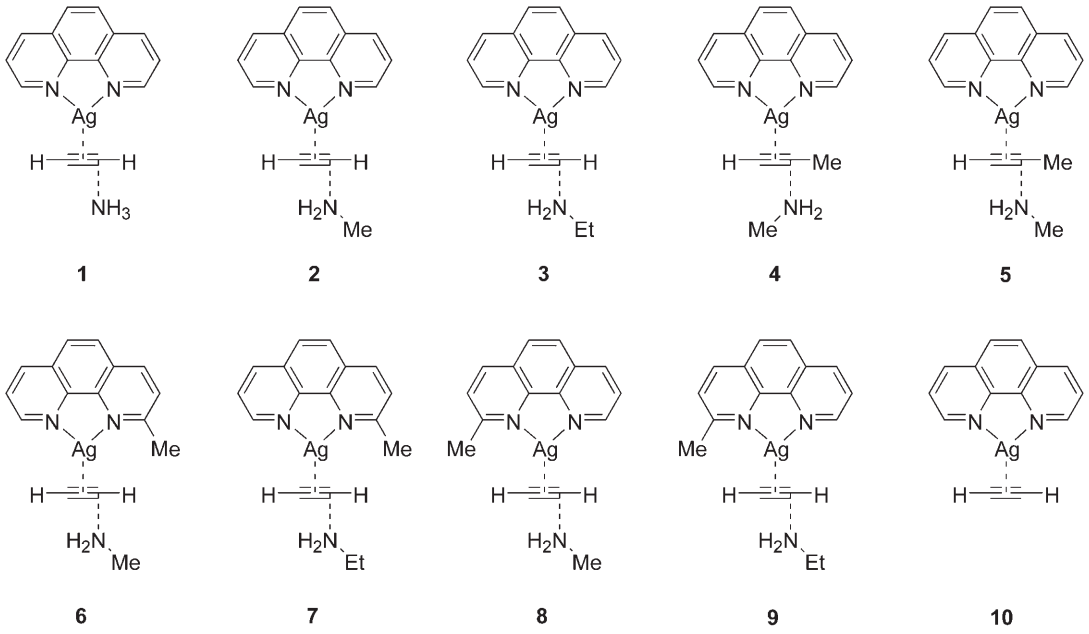

Figure 1. Transition structures **1**–**9** and ground state structure **10**.

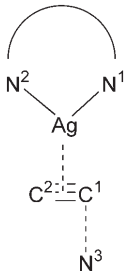

Figure 2. The catalyst and reacting atoms at the transition state requiring new parameters.

are now drastically different for the two carbons, with the average Ag–C^1 distance of 2.75 Å over the nine structures, while the other Ag–C^2 distance averages 2.22 Å. Similarly, the two phenanthroline Ag–N bond lengths are also different, with the average Ag–N^1 length 2.34 Å and the average Ag–N^2 length is 2.40 Å. The angles around the silver are also fairly constant. The average N–Ag–N angle in the transition structures is 71.8° which is only lightly smaller than in the ground state complex, where the angle is 73.7°. The C–Ag–C angle in the transition structures

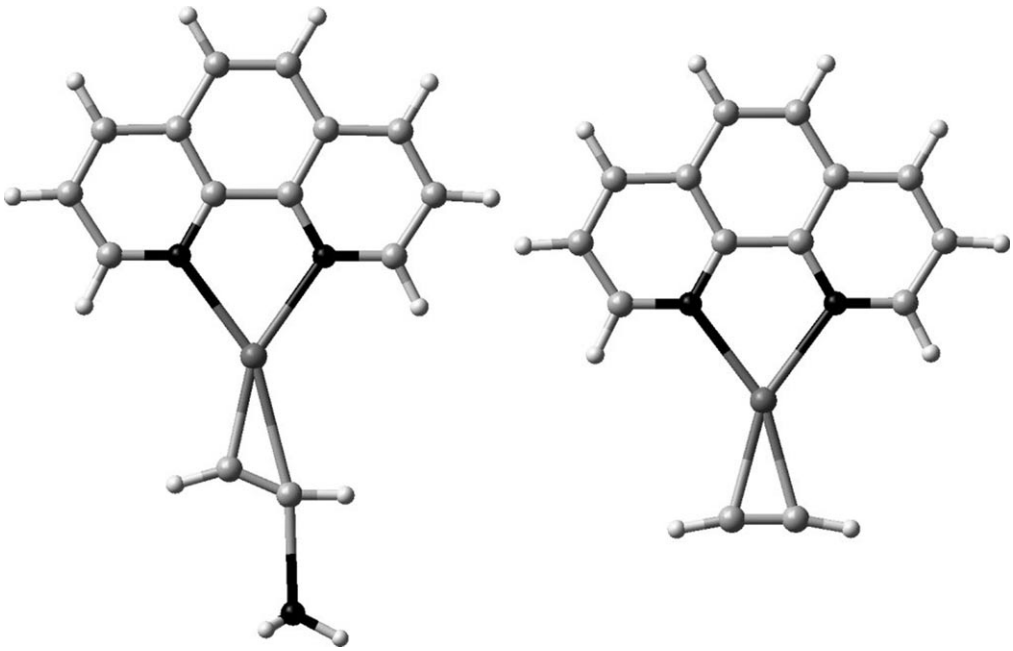

Figure 3. Calculated structures of **1** (left) and **10** (right). Atom types: C – medium gray, H – light gray, N – black, and Ag – dark gray.

Table 1. Selected bond lengths in substrates **1**–**10**. All bond lengths are given in angstroms.

Structure	Ag–C^1	Ag–C^2	Ag–N^1	Ag–N^2	C^1–C^2	C^1–N^3
1	2.74	2.21	2.35	2.40	1.25	2.27
2	2.67	2.23	2.34	2.39	1.24	2.41
3	2.68	2.23	2.34	2.39	1.24	2.42
4	2.91	2.20	2.35	2.43	1.26	2.35
5	2.93	2.20	2.36	2.43	1.26	2.28
6	2.70	2.23	2.33	2.40	1.24	2.41
7	2.72	2.23	2.33	2.41	1.24	2.40
8	2.68	2.24	2.35	2.39	1.24	2.40
9	2.68	2.24	2.35	2.39	1.24	2.41
10	2.35	2.35	2.32	2.32	1.22	–-
Average (**1**–**9**)	2.75	2.22	2.34	2.40	1.25	2.37

Table 2. Selected angles and dihedral angles in substrates **1**–**10**. All values given in degrees.

Structure	C^1–C^2–H	C^2–C^1–R	N–Ag–N	C–Ag–C	C^1–N^1–N^2–Ag	C^2–N^2–N^1–Ag
1	140.8	157.3	71.7	26.6	0.0	0.0
2	145.3	161.5	72.0	27.6	0.0	0.0
3	145.2	161.6	72.0	27.5	−1.2	−0.4
4	135.1	158.2	71.1	23.6	9.8	−2.1
5	133.7	156.3	71.0	23.3	7.7	−2.0
6	144.9	161.3	72.2	27.1	7.8	−2.2
7	144.3	161.0	72.1	26.8	−8.5	1.2
8	145.0	160.8	72.0	27.4	−8.2	2.8
9	145.1	161.1	72.1	27.5	7.5	−3.7
10	169.7	169.8	73.7	30.2	0.1	−0.1
Average (**1**–**9**)	142.2	159.9	71.8	26.4	1.7	−0.7

averages to 26.3°, which is expectedly slightly smaller than in the ground state, where the angle is 30.2°. Because the bond lengths of C^1 to the silver increases while the C^2–Ag bond shortens, the angle decreases as expected. The C^1–C^2 bond is also slightly longer in the transition state structures than in the ground state complex, with an average bond length of 1.25 Å. The lengthening of this bond suggests that the bond is transitioning from an alkyne to an alkene. This is corroborated by the decreases in the alkyne bond angles, with the average C^1–C^2–H angle being 142° and the C^2–C^1–R angle averaging 160°. The forming C^1–N^3 bond, which has no comparison in the ground state structure, was calculated to have an average length of 2.37 Å and was fairly consistent throughout all structures. The transition states are also not all planar as the ground state structure was. To quantify this planarity, the C^1–N^1–N^2–Ag and the C^2–N^2–N^1–Ag dihedral angles were measured. Transition structures **1** and **2** were calculated to be planar, and both dihedral angles were 0°. The rest of the structures had varied deviations from planarity. Structure **3**, which has a C^1–N^1–N^2–Ag dihedral angle of −1.2° and a C^2–N^2–N^1–Ag dihedral of −0.4°, showed the smallest deviation from planarity. Structures **4**, **5**, **6**, and **9** showed C^1–N^1–N^2–Ag dihedral angles ranging from 7.5° to 9.8° and C^2–N^2–N^1–Ag dihedral angles ranging from −2.0° to −3.7°. Structures **7** and **8** were calculated to have dihedral angles of a similar magnitude, but of the opposite sign, measuring −8.5° and −8.2°, respectively, for C^1–N^1–N^2–Ag and 1.2° and 2.8° for C^2–N^2–N^1–Ag. Overall, the nine transition structures show a high level of consistency about the bonds to silver, the forming C–N bond, and the changing C–C bond.

In order to calculate this system using MM methods, new parameters around the substructure shown in Figure 2 must be defined. The first set of these parameters deal with the silver. Since the MM3* parameter set that was chosen as the functional form of the force field was designed for hydrocarbons and small organic molecules, there are no parameters for transition metal atoms. Therefore, all bonds, angles, and torsions that involve the silver atom must be added to the force field. Secondly, since the system is a transition state, the forming C–N bond and changing C–C bond will be inadequately described by the parameters for ground state C–N single bonds and C≡C triple bonds, respectively. New parameters must be included for these bonds, and also any angles or torsions that encompass these bonds. In order to restrict these new parameters to only the bonds in question, and not other C–C or C–N bonds, these new parame-

ters will be put within a substructure defined in the MacroModel program. This substructure is the constant section of the molecule that is shown in Figure 2, and these new parameters will not be used elsewhere in the molecule.

The first step in adapting the force field to include this system is to add entries for any missing parameters. Within the parameter file, bonds and angles are defined by an "ideal" geometrical measurement and a force constant, with the optional addition of a dipole moment for bonds. Since the bonds and angles that are needed are fairly constant between structures, the average value for all calculated structures for the parameter is used as a starting value for the new parameter. The force constants are set at the initial values 5.0 mdyn $Å^{-1}$ for bonds and 0.5 mdyn rad^{-2} for angles. The MM3 force field uses a three-term cosine series to describe dihedral angles, and therefore the three constants for this series are included in the force field file, denoted V_1, V_2, and V_3. Initial values for these dihedrals require some chemical knowledge of the system and cannot rely on default values. Any dihedrals that may end up with three collinear atoms or that are ambiguously defined have all three constants set to zero and are not optimized. For instance, the two nitrogens in the phenanthroline cannot be distinguished based upon their bonding environment, and therefore dihedral parameters including one of these atoms are set to zero. Other dihedrals have initial values set based upon the estimated shape of the potential energy as a function of the dihedral. For example, dihedrals that would be at a minimum either eclipsed (0°) or *anti* (180°) are defined with positive values for V_2 and $V_1 = V_3 = 0$. In this reaction, the planarity, or approximate planarity, of the phenanthroline and alkyne must be described through an improper dihedral. These improper dihedrals are defined between four atoms that may not be directly bound to each other. Two examples of these improper dihedrals are the C^1–N^1–N^2–Ag and C^2–N^2–N^1–Ag dihedrals discussed earlier. A third improper dihedral was defined over C^1–C^2–N^2–N^1, but due to the ambiguity of the nitrogens, the same parameter also applies to the C^1–C^2–N^1–N^2 dihedral, which would be out of phase with the first by 180°. A dual minimum dihedral with the minima 180° apart can be described by letting V_2 dominate the parameter.

Once all of the necessary parameters were added to the force field file, the parameters were optimized to reproduce the QM through the use of Q2MM optimization method, as described previously.[5,6] Since all of the included structures were transition structures, the Hessian matrices used in the parameterization included one negative frequency and thus are a maximum in one dimension. To adapt this for a ground state force field, we used the eigenvalue inversion method proposed by Houk and coworkers.[18] Here, the Hessians were modified to replace the one negative eigenvector with a large positive value, and therefore the modified Hessians represent local minima at the transition state geometry.

The new optimized parameters are listed in the Supporting Information. Parameters used by MacroModel are defined to four decimal places. While the precision of the parameters is somewhat excessive, the parameter optimization procedure is performed within the defined input of MacroModel. The resulting parameters are reported to the level of accuracy required by the program. The dipole moments that are included are used by MacroModel to calculate atomic charges in the molecule. Therefore, the parameterization of the electrostatics is done through the refinement of a bond dipole, but the accuracy is determined through the comparison of the MM atomic charges to the QM charges calculated through electrostatic potential fitting. Due to the alteration of the Hessian during the parameterization, the force constants for bonds and angles that are involved in the reaction coordinate are significantly higher than their ground state counterparts. These large force constants result from the negative eigenvalue being replaced with a large positive value that generates a large restoring force to the transition state geometry along the reaction coordinate. In the forming C^1–N^3 bond, the bond length parameter is 2.37 Å with a force constant of 15.3374 mdyn $Å^{-1}$. This parameter is in excellent agreement with the calculated average of 2.37 Å. For comparison, the bond length parameters from the MM3 force field for a C–N single bond has a bond length of 1.38 Å and a force constant of 6.32 mdyn $Å^{-1}$. Similarly, the former alkyne bond, C^1–C^2, has a bond length parameter of 1.25 Å, which is in agreement with the calculated average bond length of 1.25 Å, and intermediate to the MM3 parameters of 1.21 Å for a C≡C triple bond and the 1.332 Å for a C=C double bond. The force constant of the C^1–C^2 bond is also quite large, 24.2141 mdyn $Å^{-1}$, compared to 15.25 mdyn $Å^{-1}$ for an alkyne and 7.50 mdyn $Å^{-1}$ for an alkene. The angles involving these bonds also have relatively large force constants. For example, the N^3–C^1–C^2 angle has a force constant of 5.4246 mdyn rad^{-2}, whereas the corresponding parameter for a normal enamine has a force constant of 0.6 mdyn rad^{-2} in the MM3* force field.[21] The new parameters for silver are within expectations from the QM data. The Ag–N bond length is 2.37 Å, which is intermediate to the 2.34 Å and 2.40 Å averages described previously. The N–Ag–N angle has a force constant of zero, therefore letting the bond lengths determine the position of the silver relative to the phenanthroline ligand. The two Ag–C distances were defined separately, with the Ag–C^1 bond having a parameter length of 2.67 Å, which is slightly shorter than the 2.75 Å average. The Ag–C^2 bond has a parameter

length of 2.27 Å, which is slightly longer than the calculated average of 2.22 Å.

The QM optimized structures were then optimized using MacroModel with the new parameters. The complexes showed general agreement, with only minor discrepancies between the structures. The QM versus MM comparison of selected bonds is shown in Table 3, and selected angles and dihedrals are shown in Table 4. The Ag–C bond lengths are in good agreement between the two methods. The Ag–C^1 bonds show a wider range of values in QM structures than in the MM structures. In previous Q2MM studies, a similar observation has been observed for bonds directly involved in the transition state; however, this steric effect was shown not to affect the relative energies, and by extension, selectivities of the reaction since any error is generally systematic.[8b] The MM calculated Ag–N bond lengths, however, are slightly longer than the QM reference bond lengths. Furthermore, the Ag–N^1 bonds are generally shorter than the Ag–N^2 bonds in the MM calculations, whereas they are longer in the QM calculations. This discrepancy is most likely caused by having a single Ag–N bond parameter in the force field and the parameter includes a fairly weak force constant (0.4186 mdyn $Å^{-1}$). The C^1–C^2 and C^1–N^3 bonds lengths are in agreement with the QM values. However, due to the high force constants associated with these new bond parameters, the values of 1.24 Å and 2.37 Å, respectively, are almost constant over all structures. Significant electronic or steric effects that may affect the lengths of these transition state bond distances may not be well reproduced by these force field parameters due to these high force constants. The selected angles in Table 4 show similar trends. The C^1–C^2–H and C^1–C^2–R angles are reproduced well, as is the C–Ag–C angle. However, since the Ag–N bonds are slightly longer in the MM calculations than in the QM structure, the N–Ag–N angle is therefore slightly smaller. The improper torsion parameters in the force field are set with V_2 being a positive value and $V_1 = V_3 = 0$, therefore setting minima at 0° and 180°. All of the structures have minimized to have the C^1–N^1–N^2–Ag and C^2–N^2–N^1–Ag dihedrals minimize to exactly zero. While the QM structures have much larger deviations from these values in some cases, the energy barrier to rotation along these improper dihedrals is set to be rather low, less than 2 kcal mol^{-1}. Deviations from planarity based on steric effects from the ligand are therefore not excluded, and the system is not constrained to be planar. Overall, the QM structures and MM structures have very good agreement. The RMSD values for the corresponding structures are shown in Table 5. For the "all atom" RMSD values,

Table 3. Comparison of QM and MM bond distances in transition structures **1**–**9** in angstroms.

Structure	Ag–C^1		Ag–C^2		Ag–N^1		Ag–N^2		C^1–C^2		C^1–N^3	
	QM	MM	QM	MM	QM	MM	QM	MM	QM	MM	QM	MM
1	2.74	2.70	2.21	2.24	2.40	2.46	2.35	2.49	1.25	1.24	2.27	2.37
2	2.67	2.70	2.23	2.24	2.39	2.46	2.34	2.49	1.24	1.24	2.41	2.37
3	2.68	2.70	2.23	2.24	2.39	2.46	2.34	2.49	1.24	1.24	2.42	2.37
4	2.91	2.79	2.20	2.19	2.43	2.47	2.35	2.48	1.26	1.24	2.35	2.37
5	2.93	2.79	2.20	2.19	2.43	2.47	2.36	2.49	1.26	1.24	2.28	2.37
6	2.70	2.70	2.23	2.24	2.40	2.42	2.33	2.55	1.24	1.24	2.41	2.37
7	2.72	2.70	2.23	2.24	2.41	2.42	2.33	2.55	1.24	1.24	2.40	2.37
8	2.68	2.70	2.24	2.24	2.39	2.52	2.35	2.44	1.24	1.24	2.40	2.37
9	2.68	2.70	2.24	2.24	2.39	2.52	2.35	2.44	1.24	1.24	2.41	2.37

Table 4. Comparison of QM and MM angles and dihedral angles in transition structures **1**–**9** in degrees.

Structure	C^1–C^2–H		C^2–C^1–R		N–Ag–N		C–Ag–C		C^1–N^1–N^2–Ag		C^2–N^2–N^1–Ag	
	QM	MM	QM	MM	QM	MM	QM	MM	QM	MM	QM	MM
1	140.8	142.0	157.3	161.0	71.7	63.1	26.6	27.2	0.0	0.0	0.0	0.0
2	145.3	142.0	161.5	161.1	72.0	63.1	27.6	27.2	0.0	0.0	0.0	0.0
3	145.2	142.0	161.6	161.0	72.0	63.1	27.5	27.2	1.2	0.0	−0.4	0.0
4	135.1	136.0	158.2	152.6	71.1	63.0	23.6	25.5	−9.8	0.0	−2.1	0.0
5	133.7	135.9	156.3	152.6	71.0	63.0	23.3	25.5	−7.7	0.0	−2.0	0.0
6	144.9	142.0	161.3	161.0	72.2	63.2	27.1	27.2	−7.8	0.0	−2.2	0.0
7	144.3	142.1	161.0	160.6	72.1	63.2	26.8	27.2	8.5	0.0	1.2	0.0
8	145.0	142.0	160.8	161.1	72.0	63.4	27.4	27.2	8.2	0.0	2.8	0.0
9	145.1	142.1	161.1	161.0	72.1	63.4	27.5	27.2	−7.5	0.0	−3.7	0.0

Table 5. RMSD values for transition state structures **1**–**9** for all atoms (full) and atoms included in new parameters (core) given in angstroms.

Structure	Full RMSD	Core RMSD	Structure	Full RMSD	Core RMSD
1	0.24	0.16	**6**	0.36	0.19
2	0.20	0.13	**7**	1.04	0.25
3	0.16	0.16	**8**	0.44	0.20
4	0.51	0.23	**9**	0.46	0.18
5	0.46	0.21			

there are some larger deviations, notably for **7**. In this case, the large deviation is caused from a dihedral rotation of the ethylamine around the forming C–N bond, and the deviations of the rest of the structure are minor. For a comparison of just the section of the molecule involving the new parameters, the "core" RMSD values are also given. These RMSD values are only for the atoms in the reactive center of the molecule described in Figure 2. The RMSD values for the core of all structures are very low, around 0.2 Å, and consistent across all structures. The new force field parameters, therefore, describe the silver-phenanthroline-catalyzed hydroamination of alkynes in agreement with the DFT calculations.

Conclusions

Using the Q2MM method, new force field parameters were developed to represent the transition state for the silver-catalyzed hydroamination of alkynes. These parameters were derived from representative DFT calculations, and are applicable for a wide range of substrates and ligands. Through use of this force field, energy differences between diastereomeric transition states can be calculated and the enantioselectivity of a reaction predicted computationally. These calculations will allow for the virtual screening of a library of ligands without the need for every ligand in the library to be synthesized or purchased, and will help to reduce the cost of optimizing an enantioselective reaction in terms of time and materials. Studies directed towards the experimental verification of these predictions using chiral silver complexes for the desymmetrization of a *meso* diyne, as described in Figure 4,[13] are currently in progress and will be reported in due course.

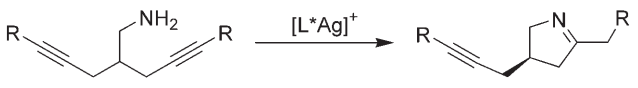

Figure 4. Desymmetrization of a *meso*-aminodiyne through an intramolecular hydroamination.

Experimental Section

Computational Methods

All electronic structure calculations were performed with Jaguar 4.2[19] using the B3LYP functional[20] together with the LACVP* basis set[21] in the gas phase. Earlier studies by our group[22] and others[23] have shown that this methodology is suitable for the calculation of silver-alkyne complexes of the type discussed here. Transition structures were located by the eigenvalue following routing implemented in Jaguar and the Hessian matrix was obtained by harmonic frequency calculations Force field calculations were performed with MacroModel[24] using an MM3* force field with additional terms generated by the Q2MM method, using geometries and Hessian matrix elements for the substructures discussed in the text. The force field fitting procedure was used as described elsewhere.[5,6]

Acknowledgements

We would like to thank Professor Per-Ola Norrby for valuable discussions and for hosting E.K. during research visits to his laboratory. We also thank the University of Notre Dame and Procter & Gamble Pharmaceuticals for support of this work.

References

[1] a) *Virtual Screening*, (Ed.: G. Klebe), Kluwer Academics, Dordrecht, **2000**; b) *Virtual Screening for Bioactive Molecules*, (Eds.: H.-J. Böhm, G. Schneider), Wiley-VCH, Weinheim, **2000**; c) P. Lyne, *Drug Discovery Today* **2002**, *7*, 1047–1055; d) *Virtual Screening in Drug Discovery*, (Eds: J. Alvarez, B. Schoichet), CRC Press, Boca Raton, FL, **2005**; e) W. L. Jorgensen *Science* **2004**, *303*, 1813–1818.

[2] a) H. Gohlke, G. Klebe, B. Waszkowycz, *Curr. Op. Drug Disc. Dev.* **2002**, *5*, 407–413; b) N. Pattabiraman, *Curr. Med. Chem.* **2002**, *9*, 609–621; c) G. Klebe *J. Mol. Med.* **2000**, *78*, 269–281; d) R. D. Taylor, P. J. Jewsbury, J. W. Essex, *J. Comp. Aid. Mol. Design* **2002**, *16*, 151–166; e) P. D. Lyne, *Drug Discovery Today* **2002**, *7*, 1047–1055.

[3] a) F. J. Jensen, *Chem. Phys.* **2003**, *119*, 8804–8808; b) A. K. Rappe, M. A. Pietsch, D. C. Wiser, J. R. Hart, L. M. Bormann-Rochotte, W. M. Skiff, *Mol. Engin.* **1997**, *7*, 385–400; c) F. Jensen, P.-O. Norrby, *Theor. Chem. Acc.* **2003**, *109*, 1–7.

[4] a) A. Bernardi, C. Gennari, J. M. Goodman, I. Paterson, *Tetrahedron: Asymmetry* **1995**, *6*, 2613–2636; b) J. E. Eksterowicz, K. N. Houk, *Chem. Rev.* **1993**, *93*, 2439–2461; c) K. B. Lipkowitz, M. A. Peterson, *Chem. Rev.* **1993**, *93*, 2463–2486; d) C. S. Ewig, R. Berry, U. Dinur, J.-R. Hill, M.-J. Hwang, H. Li, C. Liang, J. Maple, Z. Peng, T. P. Stockfisch, T. S. Thacher, L. Yan, X. Ni, A. T. Hagler, *J. Comp. Chem.* **2001**, *22*, 1782–1800.

[5] a) P.-O. Norrby, T. Liljefors, *J. Comput. Chem.* **1998**, *19*, 1146–1166; b) P.-O. Norrby, P. Brandt, *Coord. Chem. Rev.* **2001**, *212*, 79–109; c) P.-O. Norrby, in: *Computational Organometallic Chemistry*, (Ed: T. Cundari), Marcel Dekker, New York, **2001**, pp 7–37.
[6] a) P.-O. Norrby, in: *Transition State Modeling for Catalysis.* ACS Symp. Ser., American Chemical Society, Washington, DC, **1999**, No. 721, pp 163–172; b) P.-O. Norrby, *J. Mol. Struct. (THEOCHEM)* **2000**, *506*, 9–16.
[7] a) M. J. Sherrod, F. M. Menger , *J. Am. Chem. Soc.* **1989**, *111*, 2611–2613; b) F. M. Menger, M. J. Sherrod, *J. Am. Chem. Soc.* **1990**, *112*, 8071–8075.
[8] a) P.-O. Norrby, P. Brandt, T. Rein, *J. Org. Chem.* **1999**, *64*, 5845–5852; b) P.-O. Norrby, T. Rasmussen, J. Haller, T. Strassner, K. N. Houk, *J. Am. Chem. Soc.* **1999***, 121*, 10186–10192; c) T. Rasmussen, P.-O. Norrby, *J. Am. Chem. Soc.* **2003***, 125*, 5130–5138; d) P. Fristrup, D. Tanner, P.-O. Norrby, *Chirality* **2003***, 15*, 360–368; e) P. Fristrup, G. H. Jensen, M. L. N. Andersen, D. Tanner, P.-O. Norrby, *J. Organomet. Chem.* **2006***, 691*, 2182–2198; f) P. Rydberg, L. Olsen, P.-O. Norrby, U. Ryde, *J. Chem. Theory Comput.* **2007***, 3*, 1765–1773.
[9] a) D. O'Hagan, *Nat. Prod. Rep.* **2000**, *17*, 435–446; b) Y. Higashio, T. Shoji, *Appl. Catal., A* **2004**, *260*, 251–259.
[10] S. Hong, T. J. Marks, *Acc. Chem. Res.* **2004**, *37*, 673–686.
[11] I. Bytschkov, S. Doye, *Eur. J. Org. Chem.* **2003**, 935–946.
[12] M. R. Crimmin, I. J. Casely, M. S. Hill, *J. Am. Chem. Soc.* **2005**, *127*, 2042–2043.
[13] J. M. Carney, P. J. Donoghue, W. M. Wuest, O. Wiest, P. Helquist, submitted.
[14] Compare also: a) Y. Koseki, S. Kusano, S. T. Nagasaka, *Tetrahedron Lett.* **1998**, *39*, 3517–3520; b) T. E. Müller, *Tetrahedron Lett.* **1998**, *39*, 5961–5962; c) R. S. Robinson, M. C. Dovey, D. Gravestock, *Tetrahedron Lett.* **2004**, *45*, 6787–6789; d) R. S. Robinson, M. C. Dovey, D. Gravestock, *Eur. J. Org. Chem.* **2005**, 505–511; e) J. Sun, S. A. Kozmin*, Angew. Chem. Int. Ed.* **2006**, *45*, 4991–4993.
[15] J. A. Weitgenant, J. D. Mortison, D. J. O'Neill, B. Mowery, A. Puranen, P. A. Helquist, *J. Org. Chem.* **2004**, *69*, 2909–2915.
[16] T. E. Müller, J. A. Lercher, N. Van Nhu, *AIChE Journal* **2003**, *49*, 214–224.
[17] Regarding the mechanism of the reaction, compare also: D. C. Rosenfeld, S. Shekhar, A. Takemiya, M. Utsunomiya, J. F. Hartwig, *Org. Lett.* **2006**, *8*, 4179–4182.
[18] a) Wu, Y. D.; Wang, Y.; Houk, K. N. *J. Org. Chem.* **1992**, *57*, 1362–1369; b) Raimondi, L.; Brown, F. K.; Gonzalez, J.; Houk, K. N *J. Am. Chem. Soc.* **1992**, *114*, 4796–4804.
[19] Jaguar 4.2, Schrödinger, Inc., Portland, Oregon, **2000**. For the most recent version, see: http://www.schrodinger.com.
[20] a) A. D. Becke, *J. Chem. Phys.* **1993**, *98*, 5648–5652; b) C. Lee, W. Yang, R. G. Parr, *Phys. Rev. B* **1988**, *37*, 785–789.
[21] LACVP* uses the 6–31G* basis set for all light elements, and the Hay–Wadt ECP and basis set for Ag: P. J. Hay, W. R. Wadt, *J. Chem. Phys.* **1985**, *82*, 299–310.
[22] E. Kieken, O. Wiest, P. Helquist, M. E. Cucciolito, G. Flores, A. Vitagliano, P.-O. Norrby *Organometallics* **2005**, *24*, 3737–3745.
[23] R. H. Hertwig, W. Koch, D. Schroder, H. Schwarz, J. Hrusak, P. Schwerdtfeger, *J. Phys. Chem.* **1996**, *100*, 12253–12260.
[24] Macromodel 5.5: F. Mohamadi, N. G. J. Richards, W. C. Guida, R. Liskamp, M. Lipton, C. Caufield, G. Chang, T. Hendrickson, W. C. Still, *J. Comput. Chem.* **1990**, *11*, 440–467.

